# 压电纤维复合材料层合壳的非线性动力学研究*

郭翔鹰† 刘大猛 张伟

(北京工业大学机电学院, 北京 100124)

**摘要** 本文对横向激励作用下的 1-3 型压电纤维复合材料层合壳进行了非线性动力学分析,并研究了压电特性对结构振动响应的影响. 首先建立了压电纤维复合材料层合壳的非线性动力学方程,并且在已知的几何结构和材料特性基础上考虑了电场属性. 然后根据位移边界条件,选择合适的振型函数,通过 Galerkin 方法将运动控制方程转化成两自由度的非线性常微分方程. 通过数值模拟方法分析了横向激励和压电系数对压电纤维复合材料层合壳非线性振动特性的影响. 通过波形图、三维相图、庞加莱图和分叉图等来研究壳体不同类型的周期和混沌运动. 结果表明,外激励作用下结构存在复杂的非线性振动响应,同时压电参数对层合壳结构振动响应具有很强的调节作用.

**关键词** 非线性振动, 压电纤维复合材料, 悬臂壳, 压电系数

DOI: 10.6052/1672-6553-2017-004

## 引言

压电纤维复合材料(Macro Fiber Composite)是近几年兴起的一种新型压电复合材料,在振动控制、变形控制和颤振抑制等方面都有广泛的应用[1]. 压电纤维复合材料是由压电纤维粘贴于各种板壳结构表面复合而成的一种新型材料,它将压电纤维和电极以一定的方式排列在高分子聚合物的夹层中,如图 1:(1)为压电纤维层,(2)为十指交叉型电极丝,(3)为环氧聚合物. 它有寿命长、厚度薄、重量轻、韧性大和驱动力大等优点[2].

压电纤维复合材料结构同时具有驱动和传感的性能特点,这引起了国内外众多学者的极大兴趣,对压电纤维材料结构的振动特性进行了大量研究.Panda 等[3]研究了几何大变形下压电纤维增强复合材料功能梯度层合板的非线性动力学特性. Xia 等[4]基于高阶剪切变形板理论和大变形理论,分析了热环境下,表面粘结压电纤维增强复合材料驱动器的功能梯度材料板的非线性动态响应. Thinh 等[5]研究了粘结有压电驱动器和传感器贴片的玻璃纤维/聚酯复合材料板的挠曲变形和振动响应控制. Sohn 等[6]利用 Donnell 的壳理论和拉格朗日方程得到了带有压电纤维复合材料驱动器的智能材料壳结构的运动控制方程,并分析了壳体结构的动态特性. Shiyekar 等[7]基于高阶剪切变形理论,给出了双稳态情况下,压电纤维增强复合材料层合板结构振动响应的解析解. Mareishi 等[8]基于欧拉-伯努利梁理论和几何非线性理论,研究了在机械、热和电载荷共同作用下,表面粘合压电纤维增强复合材料层合梁的力学特性. 李敏等[9]研究了压电驱动器控制翼面变形方面的静动态特性. Rafee 等[10]基于一阶剪切变形板理论和几何大变形理论,研究了表面粘合压电驱动器的碳纳米管/纤维/聚合物复合材料板结构的非线性自由振动响应.

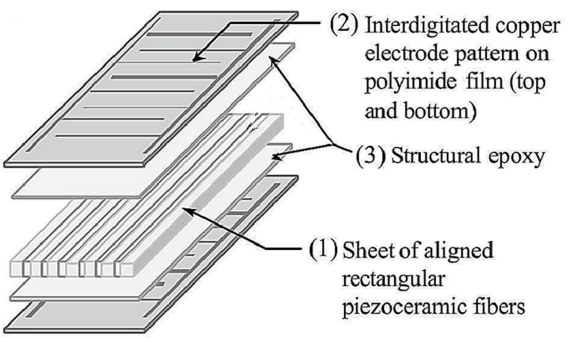


图 1 MFC 结构组成

Fig. 1 Composition of MFC structure

2016-09-27 收到第 1 稿,2016-10-24 收到修改稿.

* 国家自然科学基金(11202009, 11572006)

† 通讯作者 E-mail: eagle2008guo@yeah.net

学者们对压电材料在振动控制和结构优化等方面的应用也做了大量的研究.Sodano 等[11]研究了可充气压电纤维复合材料结构的振动抑制和结构的动态状况监测,实验结果表明将压电纤维复合材料作为传感器和致动器可以抑制结构振动. 李允等[12]采用有限元方法研究了 1-3 型压电纤维复合材料结构参数对驱动性能的影响. Ray 等[13]利用压电纤维增强复合材料做阻尼层,研究了约束层和压电纤维取向对复合材料层合薄壳振动的影响. Choi 等[14]讨论了用压电纤维复合材料驱动器来抑制旋转复合材料薄壁梁的振动响应.侯志伟等[2]研究了压电纤维复合材料的传感和驱动性能,并将其应用于梁的频响辨识和尾翼结构的减振,以及通过试验表明压电纤维复合材料有优良的传感和驱动元性能. 赵国旗等[15]有限元方法探讨了对叉指式压电纤维复合材料驱动器的结构优化.

研究压电纤维复合材料结构特性的文献较多,主要分析了压电材料在振动控制和结构优化方面的作用,大多数文献都是对薄板或者薄壳进行了研究,分析表明压电纤维材料对结构振动响应有一定的影响,而对于压电材料对中厚度板壳动力学行为的分析很少. 本文主要研究了一个 1-3 型压电纤维复合材料[16]的中厚度壳,分析了外激励的变化和压电系数的变化对壳体的非线性动力学行为的影响.

## 1　压电纤维复合材料层合壳的动力学方程

本文考虑一个正交对称铺设的 1-3 型压电纤维复合材料中等厚度的双曲壳,如图 2 所示模型,一边为固支边,其余三边自由,其在 $xy$ 面上的投影是一个矩形,长为 $a$,宽为 $b$. 曲率半径分别为 $R_1$,$R_2$,在 $\gamma$ 轴方向的厚度为 $h$.壳内的任一点在曲线坐标系内的位移分别为 $u,v,w$,横向载荷的大小为 $q=f\cos(\Omega t)$.

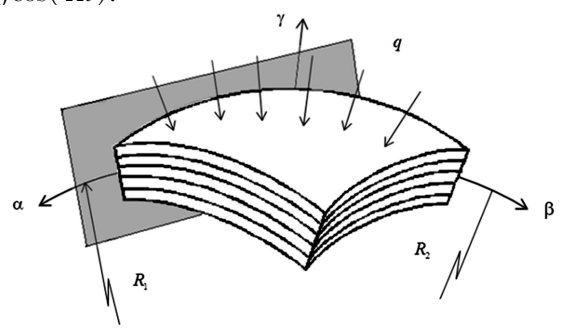


图 2　层合壳模型

Fig. 2　Model of laminated shell

采用 Reddy 的三阶剪切变形板壳理论,位移场可表示为:

$$u=u_0+\gamma\varphi_1-\frac{4}{3h^2}\gamma^3\left(\varphi_1+\frac{\partial w_0}{\partial\alpha}\right) \tag{1a}$$

$$v=v_0+\gamma\varphi_2-\frac{4}{3h^2}\gamma^3\left(\varphi_2+\frac{\partial w_0}{\partial\beta}\right) \tag{1b}$$

$$w=w_0 \tag{1c}$$

其中 $u,v,w$ 表示壳体沿着 $\alpha,\beta,\gamma$ 三个曲线坐标轴方向的位移.

采用 von Karman 的非线性几何关系可得到应变和位移的关系式如下:

$$\varepsilon_1=\frac{1}{A_1}\left(\frac{\partial u}{\partial\alpha}+\frac{1}{a_2}\frac{\partial a_1}{\partial\beta}v+\frac{a_1}{R_1}w\right)$$

$$\varepsilon_2=\frac{1}{A_2}\left(\frac{\partial v}{\partial\beta}+\frac{1}{a_1}\frac{\partial a_2}{\partial\alpha}v+\frac{a_2}{R_2}w\right)$$

$$\varepsilon_3=\frac{\partial w}{\partial\gamma}$$

$$\varepsilon_4=\frac{1}{A_2}\frac{\partial w}{\partial\beta}+A_2\frac{\partial}{\partial\gamma}\left(\frac{v}{A_2}\right)$$

$$\varepsilon_5=\frac{1}{A_1}\frac{\partial w}{\partial\alpha}+A_1\frac{\partial}{\partial\gamma}\left(\frac{u}{A_1}\right)$$

$$\varepsilon_6=\frac{A_2}{A_1}\frac{\partial}{\partial\alpha}\left(\frac{v}{A_2}\right)+\frac{A_1}{A_2}\frac{\partial}{\partial\beta}\left(\frac{u}{A_1}\right) \tag{2}$$

压电纤维复合材料本构关系的一般形式可以表示如下:

$$\sigma_p=C_{pq}\varepsilon_q-e_{kp}E_k \tag{3a}$$

$$D_i=e_{iq}\varepsilon_q+k_{ik}E_k \tag{3b}$$

其中 $E_k$ 表示电场强度,$e_{kp}$表示压电常数.

1-3 型压电纤维复合材料的应力应变关系为:

$$\begin{Bmatrix}\sigma_1\\\sigma_2\\\sigma_3\\\sigma_4\\\sigma_5\\\sigma_6\end{Bmatrix}=\begin{bmatrix}C_{11}&C_{12}&C_{13}&0&0&0\\C_{12}&C_{11}&C_{13}&0&0&0\\C_{13}&C_{13}&C_{13}&0&0&0\\0&0&0&C_{44}&0&0\\0&0&0&0&C_{44}&0\\0&0&0&0&0&\dfrac{(C_{11}-C_{12})}{2}\end{bmatrix}\begin{Bmatrix}\varepsilon_1\\\varepsilon_2\\\varepsilon_3\\\varepsilon_4\\\varepsilon_5\\\varepsilon_6\end{Bmatrix}+$$

$$\begin{bmatrix}0&0&-e_{31}\\0&0&-e_{31}\\0&0&-e_{33}\\0&-e_{15}&0\\-e_{15}&0&0\\0&0&0\end{bmatrix}\begin{Bmatrix}E_1\\E_2\\E_3\end{Bmatrix} \tag{4}$$

曲线坐标系与直角坐标系的转换关系为 $\mathrm{d}x = a_1\mathrm{d}\alpha$，$\mathrm{d}y = a_2\mathrm{d}\beta$，$\mathrm{d}z = \mathrm{d}\gamma$. 利用以上关系式可在 Hamilton 原理中直接进行坐标系的转换.应用 Hamilton 原理建立结构的非线性运动控制方程. Hamilton 原理可以表示如下：

$$\int_0^T (\delta K - \delta U + \delta V)\,\mathrm{d}t = 0 \tag{5}$$

将方程(1)、(2)、(4)代入到(6)，并展开成广义位移形式的非线性动力学方程：

$$\begin{aligned}
&a_{11}\frac{\partial^2 u_0}{\partial x^2}+a_{12}\frac{\partial^2 u_0}{\partial y^2}+a_{13}\frac{\partial^2 v_0}{\partial x\partial y}+a_{14}\frac{\partial u_0}{\partial x}+a_{15}\frac{\partial v_0}{\partial x}-\\
&a_{16}\frac{\partial u_0}{\partial y}-a_{17}\frac{\partial v_0}{\partial y}-a_{18}\frac{\partial^3 w_0}{\partial x^2}-a_{19}\frac{\partial^3 w_0}{\partial x\partial y^2}-\\
&a_{20}\frac{\partial^2 w_0}{\partial x^2}+a_{21}\frac{\partial^2 w_0}{\partial y^2}-a_{22}\frac{\partial^2 w_0}{\partial x\partial y}+a_{23}\frac{\partial w_0}{\partial x}+\\
&a_{24}\frac{\partial^2 \varphi_1}{\partial x^2}+a_{25}\frac{\partial^2 \varphi_1}{\partial y^2}+a_{26}\frac{\partial^2 \varphi_2}{\partial x\partial y}+a_{27}\frac{\partial \varphi_1}{\partial x}+a_{28}\frac{\partial \varphi_2}{\partial x}+\\
&a_{29}\frac{\partial \varphi_1}{\partial y}+a_{30}\frac{\partial \varphi_2}{\partial y}+a_{31}u_0+a_{32}\varphi_1 = I_0\ddot{u}_0
\end{aligned} \tag{6a}$$

$$\begin{aligned}
&b_{11}\frac{\partial^2 v_0}{\partial y^2}+b_{12}\frac{\partial^2 v_0}{\partial x^2}+b_{13}\frac{\partial^2 u_0}{\partial x\partial y}+b_{14}\frac{\partial v_0}{\partial y}+b_{15}\frac{\partial u_0}{\partial y}-\\
&b_{16}\frac{\partial v_0}{\partial x}-b_{17}\frac{\partial u_0}{\partial x}-b_{18}\frac{\partial^3 w_0}{\partial y^3}-b_{19}\frac{\partial^3 w_0}{\partial x^2\partial y}-\\
&b_{20}\frac{\partial^2 w_0}{\partial y^2}+b_{21}\frac{\partial^2 w_0}{\partial x^2}-b_{22}\frac{\partial^2 w_0}{\partial x\partial y}+b_{23}\frac{\partial w_0}{\partial y}+\\
&b_{24}\frac{\partial^2 \varphi_2}{\partial y^2}+b_{25}\frac{\partial^2 \varphi_2}{\partial x^2}+b_{26}\frac{\partial^2 \varphi_1}{\partial x\partial y}+b_{27}\frac{\partial \varphi_2}{\partial y}+b_{28}\frac{\partial \varphi_1}{\partial y}+\\
&b_{29}\frac{\partial \varphi_1}{\partial y}+b_{30}\frac{\partial \varphi_1}{\partial x}+b_{31}v_0+b_{32}\varphi_2 = I_0\ddot{v}_0
\end{aligned} \tag{6b}$$

$$\begin{aligned}
&-c_{11}\frac{\partial^4 w_0}{\partial x^4}-c_{12}\frac{\partial^4 w_0}{\partial y^4}-c_{13}\frac{\partial^3 w_0}{\partial x^3}-c_{14}\frac{\partial^3 w_0}{\partial y^3}-c_{15}\frac{\partial^4 w_0}{\partial x^2\partial y^2}+\\
&c_{16}\frac{\partial^3 w_0}{\partial x^2\partial y}+c_{17}\frac{\partial^3 w_0}{\partial x\partial y^2}+c_{18}\left(\frac{\partial w_0}{\partial x}\right)^2+c_{19}\frac{\partial^2 w_0}{\partial x^2}+\\
&c_{20}\left(\frac{\partial w_0}{\partial y}\right)^2+c_{21}\frac{\partial^2 w_0}{\partial y^2}+c_{22}\frac{\partial u_0}{\partial x}+c_{23}\frac{\partial v_0}{\partial y}+\\
&c_{24}\frac{\partial u_0}{\partial x}\frac{\partial^2 w_0}{\partial x^2}+c_{25}\frac{\partial^2 u_0}{\partial x^2}\frac{\partial w_0}{\partial x}+c_{26}v_0\frac{\partial^2 w_0}{\partial x^2}+\\
&c_{27}\frac{\partial v_0}{\partial x}\frac{\partial w_0}{\partial x}+c_{28}w_0\frac{\partial^2 w_0}{\partial x^2}+c_{29}\frac{\partial v_0}{\partial y}\frac{\partial^2 w_0}{\partial x^2}+\\
&c_{30}u_0\frac{\partial^2 w_0}{\partial x^2}+c_{31}\frac{\partial u_0}{\partial x}\frac{\partial w_0}{\partial x}+c_{32}\frac{\partial v_0}{\partial x}\frac{\partial^2 w_0}{\partial x\partial y}+\\
&c_{33}\frac{\partial^2 v_0}{\partial x^2}\frac{\partial w_0}{\partial y}-c_{34}u_0\frac{\partial^2 w_0}{\partial x\partial y}-c_{35}\frac{\partial u_0}{\partial x}\frac{\partial w_0}{\partial y}+\\
&c_{36}\frac{\partial u_0}{\partial y}\frac{\partial^2 w_0}{\partial x\partial y}+c_{37}\frac{\partial^2 u_0}{\partial x\partial y}\frac{\partial w_0}{\partial y}-c_{38}v_0\frac{\partial^2 w_0}{\partial x\partial y}-\\
&c_{39}\frac{\partial v_0}{\partial x}\frac{\partial w_0}{\partial y}+c_{40}\frac{\partial^2 v_0}{\partial x\partial y}\frac{\partial w_0}{\partial x}-c_{41}\frac{\partial u_0}{\partial y}\frac{\partial w_0}{\partial x}+\\
&c_{42}\frac{\partial^2 u_0}{\partial y^2}\frac{\partial w_0}{\partial x}-c_{43}\frac{\partial v_0}{\partial y}\frac{\partial w_0}{\partial x}+c_{44}\frac{\partial u_0}{\partial x}\frac{\partial^2 w_0}{\partial y^2}+\\
&c_{45}v_0\frac{\partial^2 w_0}{\partial y^2}+c_{46}\frac{\partial v_0}{\partial y}\frac{\partial w_0}{\partial y}+c_{47}w_0\frac{\partial^2 w_0}{\partial y^2}+\\
&c_{48}\frac{\partial v_0}{\partial y}\frac{\partial^2 w_0}{\partial y^2}+c_{49}\frac{\partial^2 v_0}{\partial^2 y}\frac{\partial w_0}{\partial y}+c_{50}u_0\frac{\partial^2 w_0}{\partial y^2}+\\
&c_{51}\frac{\partial u_0}{\partial y}\frac{\partial w_0}{\partial y}+c_{52}\frac{\partial^3 \varphi_1}{\partial x^3}+c_{53}\frac{\partial^3 \varphi_2}{\partial y^3}+c_{54}\frac{\partial^3 \varphi_2}{\partial x^2\partial y}+\\
&c_{55}\frac{\partial^3 \varphi_2}{\partial x\partial y^2}+c_{56}\frac{\partial^2 \varphi_2}{\partial x^2}+c_{57}\frac{\partial^2 \varphi_1}{\partial x^2}+c_{58}\frac{\partial^2 \varphi_2}{\partial y^2}+\\
&c_{59}\frac{\partial^2 \varphi_1}{\partial y^2}+c_{60}\frac{\partial^2 \varphi_1}{\partial x\partial y}+c_{61}\frac{\partial^2 \varphi_2}{\partial x\partial y}-c_{62}u_0-c_{63}v_0-\\
&c_{64}w_0+f\cos(\Omega t)-k\dot{w}_0 = c_1I_4\left(\frac{\partial \ddot{\varphi}_1}{\partial x}+\frac{\partial \ddot{\varphi}_2}{\partial y}\right)-\\
&c_1^2I_6\left[\left(\frac{\partial \varphi_1}{\partial x}+\frac{\partial \varphi_2}{\partial y}\right)+\left(\frac{\partial^2 \ddot{w}_0}{\partial x^2}+\frac{\partial^2 \ddot{w}_0}{\partial y^2}\right)\right]+I_0\ddot{w}_0
\end{aligned} \tag{6c}$$

$$\begin{aligned}
&d_{11}\frac{\partial^2 \varphi_1}{\partial x^2}+d_{12}\frac{\partial^2 \varphi_1}{\partial y^2}+d_{13}\frac{\partial \varphi_1}{\partial x}+d_{14}\frac{\partial \varphi_1}{\partial y}+\\
&d_{15}\frac{\partial \varphi_2}{\partial x}+d_{16}\frac{\partial \varphi_2}{\partial y}+d_{17}\frac{\partial^2 \varphi_2}{\partial x\partial y}+d_{18}\frac{\partial^3 w_0}{\partial x^3}+\\
&d_{19}\frac{\partial^3 w_0}{\partial x\partial y^2}+d_{20}\frac{\partial^2 w_0}{\partial x^2}+d_{21}\frac{\partial^2 w_0}{\partial y^2}+d_{22}\frac{\partial^2 w_0}{\partial x\partial y}+\\
&d_{23}\frac{\partial w_0}{\partial x}+d_{24}u_0+d_{25}\varphi_1 = I_2\ddot{\varphi}_1-c_1I_4\ddot{\varphi}_1-\\
&c_1I_4\frac{\partial \ddot{w}_0}{\partial x}+c_1\left(-I_4\ddot{\varphi}_1-c_1I_6\ddot{\varphi}_1+c_1I_6\frac{\partial \ddot{w}_0}{\partial x}\right)
\end{aligned} \tag{6d}$$

$$\begin{aligned}
&e_{11}\frac{\partial^2 \varphi_2}{\partial y^2}+e_{12}\frac{\partial^2 \varphi_2}{\partial x^2}+e_{13}\frac{\partial \varphi_2}{\partial y}+e_{14}\frac{\partial \varphi_2}{\partial x}+\\
&e_{15}\frac{\partial \varphi_1}{\partial y}+e_{16}\frac{\partial \varphi_1}{\partial x}+e_{17}\frac{\partial^2 \varphi_1}{\partial x\partial y}+e_{18}\frac{\partial^3 w_0}{\partial y^3}+\\
&e_{19}\frac{\partial^3 w_0}{\partial x^2\partial y}+e_{20}\frac{\partial^2 w_0}{\partial y^2}+e_{21}\frac{\partial^2 w_0}{\partial x^2}+e_{22}\frac{\partial^2 w_0}{\partial x\partial y}+\\
&e_{23}\frac{\partial w_0}{\partial y}+e_{24}v_0+e_{25}\varphi_2 = I_2\ddot{\varphi}_2-c_1I_4\ddot{\varphi}_2-\\
&c_1I_4\frac{\partial \ddot{w}_0}{\partial y}+c_1\left(-I_4\ddot{\varphi}_2-c_1I_6\ddot{\varphi}_2+c_1I_6\frac{\partial \ddot{w}_0}{\partial y}\right)
\end{aligned} \tag{6e}$$

其中,$c_1=\dfrac{4}{3h^2}$, $c_2=3c_1$,$k$ 为横向振动阻尼系数,$f$ 是外激励幅值.

悬臂壳的边界条件为:

$$x=0:\ N_{xy}=M_{xx}=M_{xy}-c_1P_{xy}=\overline{Q}_x=0 \tag{7a}$$

$$x=a:\ N_{xy}=M_{xx}=M_{xy}-c_1P_{xy}=\overline{Q}_x=0 \tag{7b}$$

$$y=0:\ u_0=v_0=w_0=\varphi_1=\varphi_2=0 \tag{7c}$$

$$y=b:\ N_{yy}=N_{xy}=M_{yy}=M_{xy}-c_1P_{xy}=\overline{Q}_y=0 \tag{7d}$$

$$\int_{-\frac{h}{2}}^{\frac{h}{2}}N_{xx}\mathrm{d}z=\pm\int_{-\frac{h}{2}}^{\frac{h}{2}}f\mathrm{d}z,(x=0,a) \tag{7e}$$

结构的刚度系统可以表示为:

$$(A_{ij},B_{ij},D_{ij},E_{ij},F_{ij},H_{ij})=\sum_{k=1}^{N}\int_{\gamma_k}^{\gamma_{k+1}}\overline{Q}_{ij}^{k}(1,\gamma,\gamma^2,\gamma^3,\gamma^4,\gamma^6)d\gamma\quad(i,j=1,2,6)$$

$$(A_{ij},D_{ij},F_{ij})=\sum_{k=1}^{N}\int_{\gamma_k}^{\gamma_{k+1}}\overline{Q}_{ij}^{k}(1,\gamma^2,\gamma^4)d\gamma\quad(i,j=4,5) \tag{8a}$$

$$I_i=\int_{-h/2}^{h/2}\rho\gamma^i d\gamma\quad(i=0,1,2,3,4,6) \tag{8b}$$

## 2　Galerkin 离散

将动力学方程无量纲化后,可得到结构无量纲形式的动力学方程. 通过 Galerkin 方法将系统的非线性运动控制方程离散,根据边界条件选取如下模态形式:

$$u_0=u_1\sin\frac{\pi x}{2}\cos\pi y+u_2\sin\frac{3\pi x}{2}\cos2\pi y \tag{9a}$$

$$v_0=v_1\sin\frac{\pi x}{2}\sin\pi y+v_2\sin\frac{3\pi x}{2}\sin2\pi y \tag{9b}$$

$$\varphi_1=\varphi_{11}\sin\frac{\pi x}{2}\cos\pi y+\varphi_{12}\sin\pi x\cos2\pi y \tag{9c}$$

$$\varphi_2=\varphi_{21}\left(1-\cos\frac{\pi x}{2}\right)\sin\pi y+\varphi_{22}\left(1-\cos\frac{\pi x}{2}\right)\sin2\pi y \tag{9d}$$

$$w_0=w_1(t)X_1(x)Y_1(y)+w_2(t)X_2(x)Y_2(y) \tag{9e}$$

其中,

$$X_i(x)=\sin\lambda_i x-\sinh\lambda_i x+\alpha_i(\cosh\lambda_i x-\cos\lambda_i x) \tag{10a}$$

$$Y_1(y)=1 \tag{10b}$$

$$Y_2(y)=\sqrt{3}\left(1-\frac{2y}{b}\right) \tag{10c}$$

$$\cos\lambda_i a\cosh\lambda_i a+1=0 \tag{10d}$$

$$\cos\mu_j b\cosh\mu_j b-1=0 \tag{10e}$$

$$\alpha_i=\frac{\sinh\lambda_i a+\sin\lambda_i a}{\cosh\lambda_i a+\cos\lambda_i a} \tag{10f}$$

由于所建立的中厚度复合材料壳结构动力学模型中,横向振动比其他两个方向的振动要大很多,所以本文重点研究结构的横向振动特性,将离散后的方程简化得到两自由度非线性动力学方程如下:

$$\ddot{w}_1+\mu\dot{w}_1+\omega_1^2w_1+\alpha_{11}w_1^2+\alpha_{12}w_2^2+\alpha_{13}w_1w_2+\alpha_{14}w_1\cos\Omega_2t++\alpha_{15}w_2\cos\Omega_2t=\alpha_{16}f\cos\Omega_1t \tag{11a}$$

$$\ddot{w}_2+\mu\dot{w}_2+\omega_2^2w_2+\alpha_{21}w_1^2+\alpha_{22}w_2^2+\alpha_{23}w_1w_2+\alpha_{24}w_1\cos\Omega_2t+\alpha_{25}w_2\cos\Omega_2t=\alpha_{26}f\cos\Omega_1t \tag{11b}$$

其中,$\mu$ 为阻尼系数,$\alpha_{14}$,$\alpha_{15}$,$\alpha_{24}$,$\alpha_{25}$为压电系数.

## 3　摄动分析

采用多尺度法对偏微分方程进行摄动分析,引入小参数 $\varepsilon$,并设方程的解为:

$$w_1=w_{10}(T_0,T_1)+\varepsilon w_{11}(T_0,T_1)+\cdots \tag{12a}$$

$$w_2=w_{20}(T_0,T_1)+\varepsilon w_{21}(T_0,T_1)+\cdots \tag{12b}$$

其中,$T_0=t$,$T_1=\varepsilon t$.

微分算子为:

$$\frac{d}{dt}=D_0+\varepsilon D_1 \tag{13a}$$

$$\frac{d^2}{dt^2}=D_0^2+2\varepsilon D_0D_1 \tag{13b}$$

本文分析系统主参数共振和 1∶1内共振的情况,建立相应的关系如下:

$$\omega_1^2=\Omega_1^2+\varepsilon\sigma_1$$

$$\omega_2^2=\Omega_1^2+\varepsilon\sigma_2$$

$$\omega_1^2\approx\omega_2^2$$

$$\Omega_1=\Omega_2=1 \tag{14}$$

其中,$\sigma_1$、$\sigma_2$ 是调谐参数.

将方程(12)、(13)和(14)代入方程(11),令方程两边 $\varepsilon$ 同阶项系数相等,则得微分方程如下:

$\varepsilon^0$ 阶:

$$D_0w_{10}+\Omega_1^2w_{10}=0 \tag{15a}$$

$$D_0w_{20}+\Omega_1^2w_{20}=0 \tag{15b}$$

$\varepsilon^1$ 阶:

$$D_0w_{11}+\Omega_1^2w_{11}=-2D_0D_1w_{10}-\mu D_0w_{10}-\sigma_1w_{10}-$$

$$\alpha_{11}w_{10}^2-\alpha_{12}w_{20}^2-\alpha_{13}w_{10}w_{20}-\alpha_{14}w_{10}\cos\Omega_2 t-\alpha_{15}w_{20}\cos\Omega_2 t+\alpha_{16}f\cos\Omega_1 t \tag{16a}$$

$$D_0w_{21}+\Omega_1^2w_{21}=-2D_0D_1w_{20}-\mu D_0w_{20}-\sigma_1w_{20}-\alpha_{21}w_{10}^2-\alpha_{22}w_{20}^2-\alpha_{23}w_{10}w_{20}-\alpha_{24}w_{10}\cos\Omega_2 t-\alpha_{25}w_{20}\cos\Omega_2 t+\alpha_{26}f\cos\Omega_1 t \tag{16b}$$

设方程(15)有如下形式的解:

$$w_{10}=A(T_1)e^{i\omega T_0}+\overline{A}(T_1)e^{-i\omega T_0} \tag{17a}$$

$$w_{20}=B(T_1)e^{i\omega T_0}+\overline{B}(T_1)e^{-i\omega T_0} \tag{17b}$$

其中,$A=\frac{1}{2}a_1e^{i\theta_1}$,$B=\frac{1}{2}a_2e^{i\theta_2}$.

将方程(17)代入到方程(16)中得到系统 1∶1 内共振情况下极坐标形式的平均方程为:

$$\dot{a}_1=-\frac{1}{2}\mu a_1+\frac{1}{2}\alpha_{16}f\sin\theta_1 \tag{18a}$$

$$a_1\dot{\theta}_1=\frac{1}{2}\sigma_1a_1+\frac{1}{4}\alpha_{14}a_1+\frac{1}{4}\alpha_{15}a_2-\frac{1}{2}\alpha_{16}f\cos\theta_1 \tag{18b}$$

$$\dot{a}_2=-\frac{1}{2}\mu a_2+\frac{1}{2}\alpha_{26}f\sin\theta_2 \tag{18c}$$

$$a_2\dot{\theta}_2=\frac{1}{2}\sigma_2a_2+\frac{1}{4}\alpha_{24}a_1+\frac{1}{4}\alpha_{25}a_2-\frac{1}{2}\alpha_{26}f\cos\theta_2 \tag{18d}$$

## 4 数值模拟

本节将通过数值模拟方法研究复合材料壳结构的非线性动力学行为,研究压电系数及外激励幅值对壳体振动响应的影响. 选定一组初始参数为 $\mu=0.4$,$\alpha_{11}=29.2$,$\alpha_{12}=-6.7$,$\alpha_{13}=10.7$,$\alpha_{14}=1.0$,$\alpha_{15}=1.0$,$\alpha_{16}=25.3$,$\alpha_{21}=27.7$,$\alpha_{22}=5.2$,$\alpha_{23}=27.0$,$\alpha_{24}=1.0$,$\alpha_{25}=1.0$,$\alpha_{26}=6.9$,$x_1=1.6$,$x_2=0.3$,$x_3=1.9$,$x_1=0.9$. 方程(18)与(11)的系数有对应关系,根据方程(18),改变压电系数 $\alpha_{14}$,分别取 0.5,1.0,1.5 可以得到幅频响应曲线,如图 3 所示,横轴表示失谐参数,纵轴表示第一阶和第二阶振幅. 从图中可以看出,增大压电参数,会使得系统的刚度变小.

固定上述的参数值和初始条件,研究外激励幅值的变化对结构振动响应的影响以及压电系统对结构振动响应的调节作用,根据方程(11),改变外激励 $f$ 的幅值,研究系统的振动响应随外激励幅值的变化情况,当幅值从 300 变化到 2000 的过程中,得到壳体横向位移的分叉图,如图 4 所示. 从分叉图中分析可得,系统分别在 400、700、1550 附近出现了周期运动,而在其他的区域都为混沌运动. 图 5 给出了外激励幅值为 850 时系统的混沌运动形态.

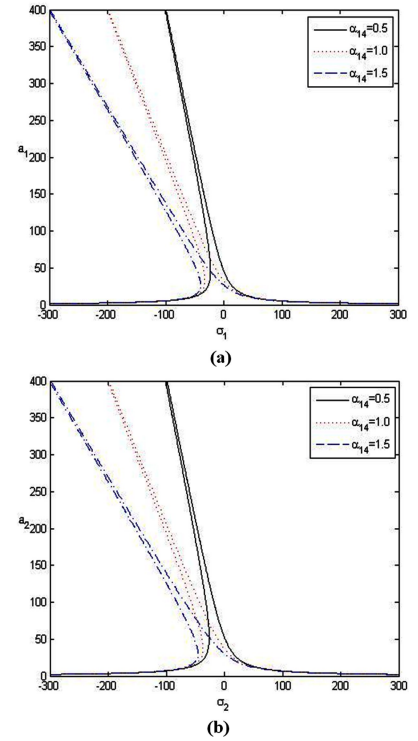


图 3 幅频响应曲线

Fig. 3 Amplitude frequency response curves

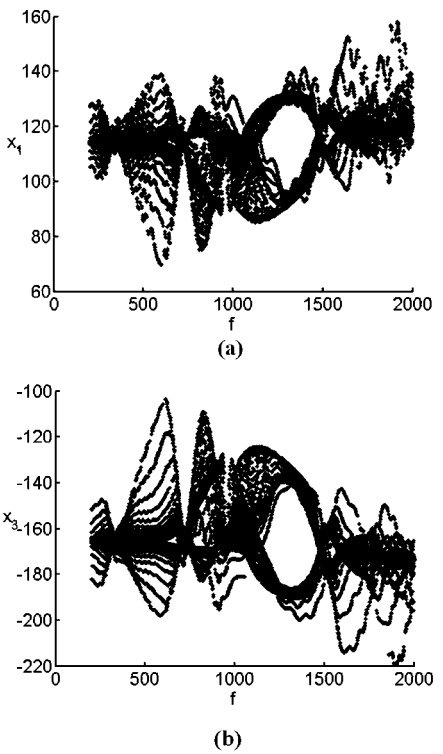


图 4 分叉图

Fig. 4 Bifurcation diagram

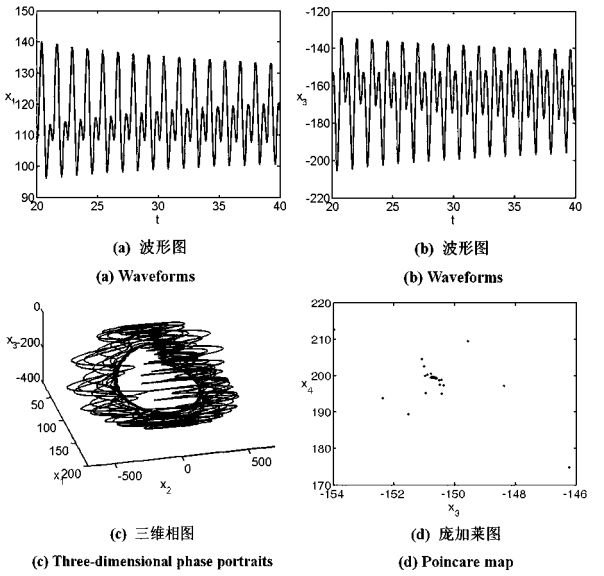


图 5　混沌运动

Fig. 5　Chaotic motion

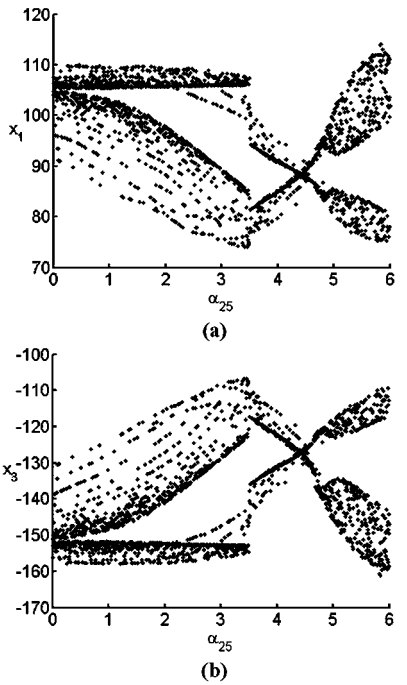


图 6　分叉图

Fig. 6　Bifurcation diagram

根据以上分析结果发现,外激励的幅值对结构振动特性的影响较大,在此基础上,通过改变结构的压电参数来调节结构的振动响应,实现压电参数对结构振动响应的抑制. 根据图 5 中的参数取值,取定激励 $f$ 的幅值为 850,只改变压电系数 $\alpha_{25}$ 的大小,可以发现当 $\alpha_{25}$ 从 0 增加到 6 的过程中,系统出现了不同的运动状态,如图 6 所示,从分叉图中看出通过改变压电系数可改变系统的非线性振动响应. 当 $\alpha_{25}$ 从 0 增加为 4.5,系统由混沌运动变为周期运动,具体的形态如图 7 所示.

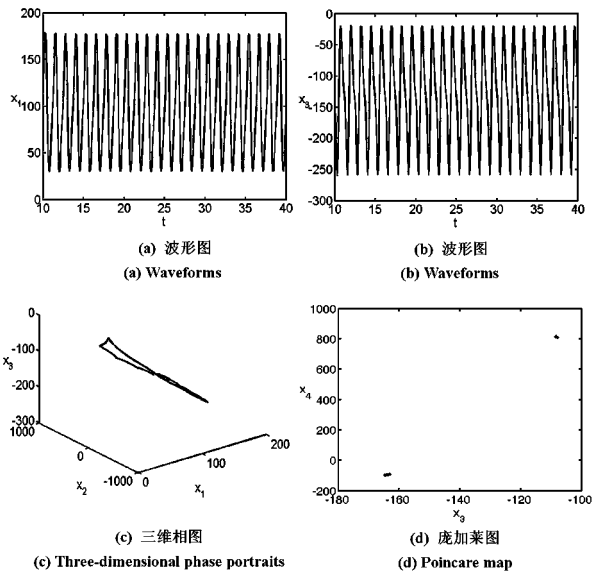


图 7　周期运动

Fig. 7　Periodic motion

为了更好地说明压电参数对系统振动响应的调节作用,再选取下面一组数据 $\mu=0.6$, $\alpha_{11}=-5.3$, $\alpha_{12}=8.9$, $\alpha_{13}=26.4$, $\alpha_{14}=1.0$, $\alpha_{15}=1.0$, $\alpha_{16}=19.3$, $\alpha_{21}=-10.4$, $\alpha_{22}=7.4$, $\alpha_{23}=-22.4$, $\alpha_{24}=1.0$, $\alpha_{25}=1.0$, $\alpha_{26}=14.1$, $x_1=2.6$, $x_2=1.3$, $x_3=4.5$, $x_1=5.1$. 如图 8 所示,当激励幅值从 3 增大到 20 的过程中,系统出现了先周期运动后混动运动. 如图9和图10给出

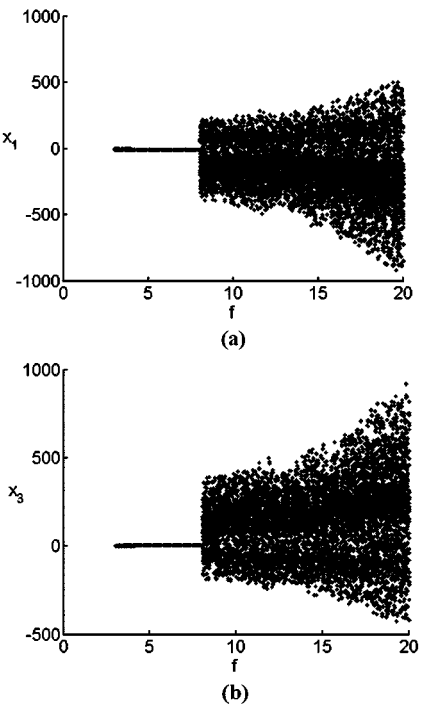


图 8　分叉图

Fig. 8　Bifurcation diagram

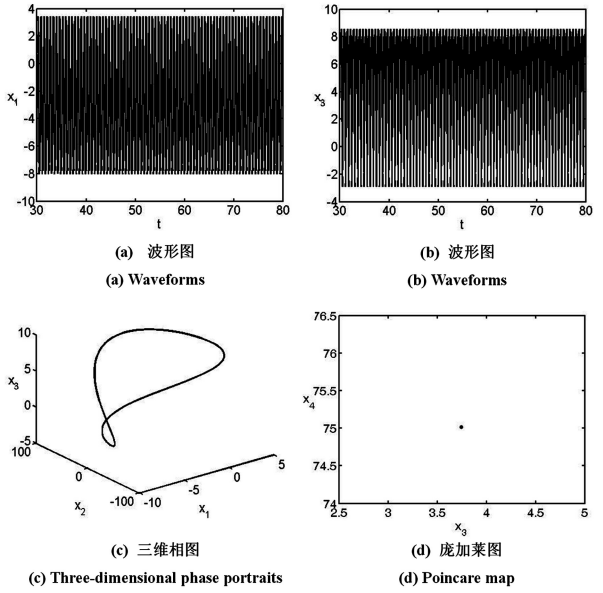


图 9 周期运动

Fig. 9 The periodic motion

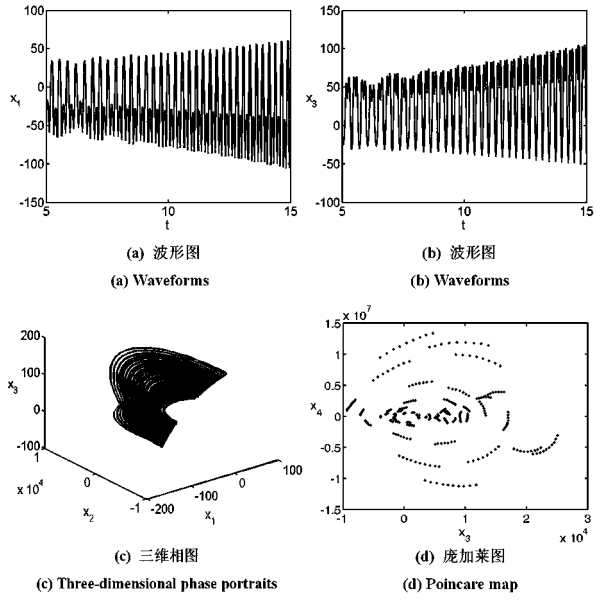


图 10 混沌运动

Fig. 10 The chaotic motion

了外激励幅值为 5 和 12 时,系统周期运动和混沌运动的具体形态.

保持上述参数不变,取定外激励 $f$ 的幅值为 12,只改变 $\alpha_{25}$的大小,系统同样出现了先混沌再周期再到混沌的运动形式. 从分叉图 11 中可以发现,当 $\alpha_{25}$从 1.0 改变为 2.0,结构原来的混沌运动将转变为周期运动,从而抑制了结构的振动响应,图 12 给出了调节后周期运动的具体形态. 通过上述两组不同的参数模拟结果可以发现,压电纤维可以起到调节和抑制结构振动响应的特性.

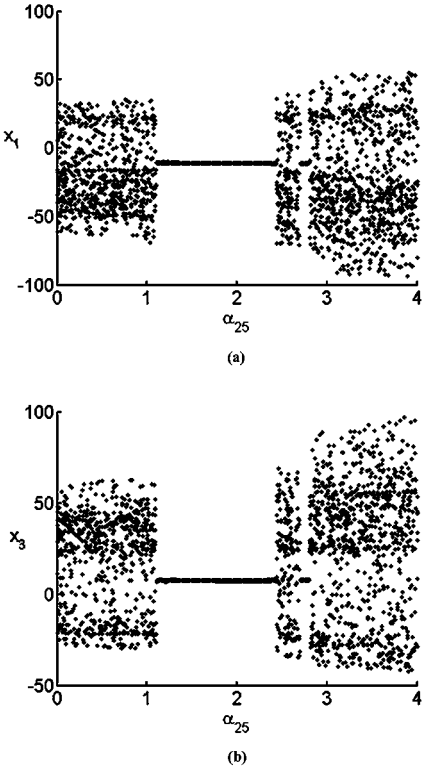


图 11 分叉图

Fig. 11 Bifurcation diagram

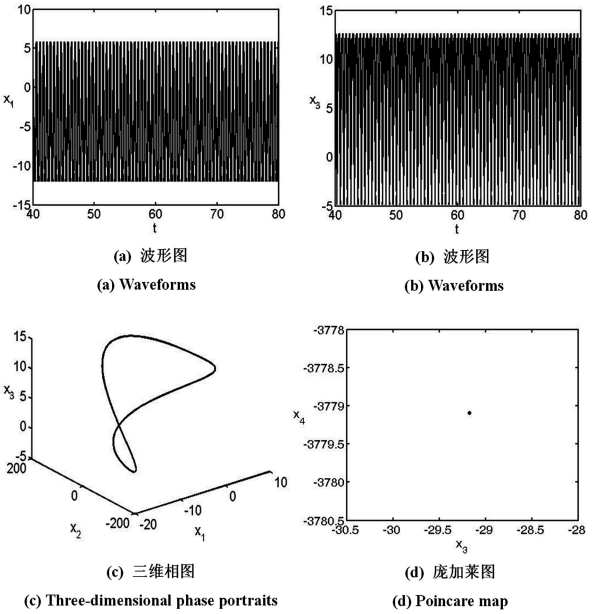


图 12 周期运动

Fig. 12 The periodic motion

## 5 结论

本文利用 Reddy 的高阶剪切理论、von Karman 大变形理论和 Hamilton 原理建立了压电纤维复合材料层合壳在横向激励作用下的非线性偏微分运

动控制方程,运用 Galerkin 方法离散得到了结构常微分形式的运动控制方程,摄动分析得到了系统极坐标形式的平均方程,并用数值方法研究了压电纤维复合材料层合壳结构在不同参数作用下的非线性动力学行为.

数值结果得到了结构在横向激励作用下幅频响应曲线以及位移的分叉图、相图、波形图和庞加莱图,在确定几何和材料参数的情况下,外激励的变化和压电系数的变化会引起结构振动响应的变化,出现从混沌到周期再到混沌的运动,通过改变压电系数可以抑制结构的振动响应. 在确定外激励幅值的情况下,改变压电系数,会改变系统的刚度,进而会改变系统的固有频率,因此压电效应会对系统的非线性振动响应产生影响. 所以,通过调节结构横向激励幅值和压电系数可以控制压电纤维复合材料层合壳结构的非线性振动响应.

## 参 考 文 献


1 李敏,陈伟民,贾丽杰. 压电纤维复合材料铺层用于翼面设计的驱动特性与刚度影响. 航空学报, 2010,31(2):418~425 (Li M, Chen W M, Jia L J. Drive characteristics and stiffness influence with piezoelectric fiber composite actuators on airfoil surface. *Acta Aeronautica et Astronautica Sinica*, 2010, 31(2): 418 ~ 425 (in Chinese))

2 侯志伟,陈仁文,徐志伟等. 压电纤维复合材料在结构减振中的应用. 振动、测试与诊断, 2010,30(1):51~54 (Hou Z W, Chen R W, Xu Z W, et al. Application of macro-fiber composite to structural vibration suppression. *Journal of Vibration, Measurement & Diagnosis*, 2010,30(1):51~54(in Chinese))

3 Panda S, Ray M C. Active control of geometrically nonlinear vibrations of functionally graded laminated composite plates using piezoelectric fiber reinforced composites. *Journal of Sound and Vibration*, 2009,325:186~205

4 Xia X K, Shen H S. Nonlinear vibration and dynamic response of FGM plates with piezoelectric fiber reinforced composite actuators. *Composite Structures*, 2009,90:254~262.

5 Thinh T, Ngoc L K. Static behavior and vibration control of piezoelectric cantilever composite plates and comparison with experiments. *Computational Materials Science*, 2010,49:S276~S280

6 Sohn J W, Choi S B, Kim H S. Vibration control of smart hull structure with optimally placed piezoelectric composite actuators. *International Journal of Mechanical Sciences*, 2011,53:647~659

7 Shiyekar S M, Kant T. Higher order shear deformation effects on analysis of laminates with piezoelectric fiber reinforced composite actuators. *Composite Structures*, 2011, 93:3252~3261

8 Mareishi S, Rafiee M, He X Q, et al. Nonlinear free vibration post buckling and nonlinear static deflection of piezoelectric fiber-reinforced laminated composite beams. *Composites: Part B*, 2014,59:123~132

9 李敏,陈伟民,贾丽杰. 压电驱动器的气动弹性应用. 航空学报, 2009,30:2301~2310 (Li M, Chen W M, Jia L J. Application of piezoelectric actuators to aircraft aeroelastic performance enhancement. *Acta Aeronautica et Astronautica Sinica*, 2009, 30: 2301 ~ 2310 (in Chinese))

10 Rafiee M, Liu X F, He X Q, et al. Geometrically nonlinear free vibration of shear deformable piezoelectric carbon nanotube/fiber/polymer multi-scale laminated composite plates. *Journal of Sound and Vibration*, 2014,333:3236~3251

11 Sodano H, Park A G, Inman D J. An investigation into the performance of macro-fiber composites for sensing and structural vibration applications. *Mechanical Systems and Signal Processing*, 2004,18:683~697

12 李允,沈星,王宁. 1-3 型压电纤维复合材料结构参数对驱动性能的影响. 材料导报, 2008,22(12):89~99 (Li Y, Shen X, Wang N. Influence of structure parameters of 1-3 piezoelectric fiber composites on actuation capability. *Materials Review*, 2008, 22(12): 89 ~ 99 (in Chinese))

13 Panda S, Ray M C. Active control of laminated cylindrical shells using piezoelectric fiber reinforced composites. *Composites Science and Technology*, 2005,65:1226~1236

14 Choi S C, Park J S, Kim J H. Active damping of rotating composite thin-walled beams using MFC actuators and PVDF sensors. *Composite Structures*, 2006,76:362~374

15 赵国旗,韩伟,骆英. 指式压电纤维复合材料驱动器的结构优化. 陶瓷学报, 2013,34(4):467~471 (Zhao G Q, Han W, Luo Y. Structure optimization of IDE piezoelectric fiber composites actuators. *Journal of Ceramics*, 2013,34(4):467~471 (in Chinese))

16 赵寿根,程伟. 1-3 型压电复合材料及其研究进展. 力

学进展, 2002,32(1):57~68 (Zhao S G, Cheng W. 1-3type piezoelectric fiber composites and their research progress. *Advances in Mechanics*, 2002,32(1):57~68 (in Chinese))

# NONLINEAR DYNAMIC ANALYSIS OF PIEZOELECTRIC MACRO-FIBER COMPOSITE LAMINATED SHELLS*

Guo Xiangying† Liu Damen Zhang Wei

(*College of Mechanical Engineering*, *Beijing University of Technology*, *Beijing* 100124, *China*)

**Abstract** This paper presents the nonlinear dynamical analysis of a multilayer d31 piezoelectric macro-fibre composite (MFC) laminated shell under the transverse excitations, and the effect of the piezoelectric properties on structure vibration response is also studied. The nonlinear dynamic equations of the MFC laminated shell is firstly established. Based on the known geometrical and material properties of its constituents, their electric field dependence was presented. The vibration mode-shape functions are then obtained according to the displacement boundary conditions, and the Galerkin method is employed to transform the partial differential equation into two nonlinear ordinary differential equations. Subsequently, numerical simulation examines the effect of the transverse excitations and the piezoelectric coefficients on the nonlinear vibration of MFC laminated shell. The two-dimensional phase portraits, three-dimensional phase portraits, waveform phase, frequency spectrum phase, and bifurcation diagram are presented and used to investigate the different kinds of the periodic and chaotic motions of (MFC) laminated shell. The results indicate that piezoelectric parameters have a strong effect on the vibration response of the MFC laminated shell.

**Key words** nonlinear vibrations, macro fiber composites, cantilever shell, piezoelectric parameter

Received 27 September 2016, revised 24 October 2016.

* The project supported by the National Natural Science Foundation of China (11202009, 11572006)

† Corresponding author E-mail: eagle2008guo@yeah.net